MODELING AND SIMULATION OF A HYDRAULIC EXCAVATOR

Juma Yousuf Alaydi

Assistant Professor, Industrial Eng. Dept., IUG, Palestine
jalaydi@mail.iugaza.edu.

ABSTRACT

The key accomplishments of this paper include characterization of hydraulic excavator formation interaction, development of hydraulic excavator kinematics and dynamics, and development of hydraulic excavator simulation models. The mathematical methods were used to (i) develop excavator's kinematics and dynamics, and (ii) establish the relationship between excavator parameters and the resistive forces from the material formation during excavation process. The SIMULATION-X simulation environment was used to develop the hydraulic excavator virtual prototypes. Two numerical examples were included to test the theoretical hypotheses and the obtained results were discussed.

KEYWORDS
Mathematical modeling, Simulation, Kane equations**,** Hydraulic excavator.

نمذجة ومحاكاة حفار هيدروليكي

جمعة يوسف العايدي أستاذ مساعد في كلية الهندسة
الجامعة الإسلامية- غزة
jalaydi@mail.iugaza.edu

الإنجازات الرئيسية لهذه الورقة تتضمن توصيف حفار هيدروليكي وتأثير الأجزاء الرئيسية للحفار على بعضها ، وانجاز كينماتيكا الحفار الهيدروليكي وديناميكيته ، وتطوير نماذج محاكاة للحفار الهيدروليكي. و التمثيل الرياضي استخدم لانجاز ما يلي:(ا) انجاز كينماتيكا الحفار الهيدروليكي وديناميكيته ، و (ب) تحديد معالم العلاقة بين الحفار ومقاومة المواد في عملية الحفر. و قد تم استخدام SimulationX لتطوير نماذج افتراضية للحفار الهيدروليكي. اثنين من الأمثلة العددية أدرجت لاختبار الفرضيات النظرية والحصول على النتائج

1- INTRODUCTION

Current technological needs in areas ranging from robotics to spacecraft design require efficient algorithms for the formulation of equations of motion for mechanical systems consisting of interconnected point masses and rigid bodies. A procedure developed by Kane & Levinson 1985; Kane et al. 1983 has achieved notable success in carrying out this task. Because of the classical nature of the subject, it is not surprising that claims for new developments can lead to considerable controversy. This has indeed occurred in regard to Kane formulation in terms of what has come to be known as Kane equations. Despite such controversy, author believes that Kane procedure is both new and insightful, especially if it is also associated with a number of auxiliary definitions that Kane has introduced for the task of dynamic analysis

Research on machine kinematics and dynamics is a key to understanding and improving their operating performance, as outlined by previous researchers. Daneshmend et al. (1993) applied the Newton-Euler method to build excavator simulation model. Tafazoli et al. (1999) developed a method to identify inertial parameters for excavator arms. Craig (1986) introduced a basic method to describe the position and orientation of components and to analyze the kinematics of the associated mechanism. Murray et al (1993) formulated the exponential method for robotic motion, which allows for a comprehensive description and analysis of the kinematic configuration in a global frame system. Kane and Levinson (1985) developed the Kane method and explained its advantages over other methods for dynamic analysis. Other researchers have used this method to analyze the dynamics of different systems such as automobiles, robotic and production machinery. Through the Kane method, a reasonable number of equations can be obtained to capture the system dynamics while avoiding many derivative processes. In addition, this method can also deal with non-holonomic constrained problems. Frimpong, et. al (2002) and Frimpong, et. al (2003) advanced excavator dynamics to simulate the excavator boom-dipper-teeth interactions with in-situ formation and muck-pile.

The essential concept of forward kinematics animation is that the positions of particular parts of the model at a specified time are calculated from the position and orientation of the object, together with any information on the joints of an articulated model. Forward kinematic animation can be distinguished from inverse kinematic animation by this means of calculation -

in inverse kinematics the orientation of articulated parts is calculated from the desired position of certain points on the model. It is also distinguished from other animation systems by the fact that the motion of the model is defined directly by the animator - no account is taken of any physical laws that might be in effect on the model, such as gravity or collision with other models [Koivo, A.J., 1994].

Ground excavation constitutes a significant component of production costs in any surface mining operation. The excavation process entails material digging and removal in which the equipment motion is constrained by the workspace geometry. A major excavation problem is the variability of material properties, resulting in varying mechanical energy input and stress loading of excavator dipper- and- tooth assembly across the working bench. This variability has a huge impact on the excavator dipper and tooth assembly in hard formations [Blouin, et. al, 2001].

In this paper, analysis of the excavator was performed by applying the Newton-Euler equations and Kane method. With the advent of computer applications, a new technology called virtual prototyping is receiving wide application in various industries. It can realistically simulate the full-motion behavior of complex mechanical systems and provide quick analysis for multiple design variations toward an optimal design. This reduces the number of costly physical prototypes, improves design quality, and dramatically reduces product development time. Additionally, the solutions to above mentioned complex equations and the corresponding analysis can be easily carried out in a virtual simulation environment. A hydraulic excavator was modeled using SIMULATION-X simulation environment. Only the front-end assembly including handle and bucket of the excavator is modeled because this paper is only concerned with the digging section of a duty cycle. Therefore, the rotation of the upper structure is not modeled and the handle and bucket assembly only moves on the vertical plane. Also, no joint friction is considered.

1. MATHEMATICAL MODELING OF A HYDRAULIC EXCAVATOR

The basic components of a hydraulic excavator used throughout this paper are shown in Figure1. The hydraulic excavator consists of an upper structure, an undercarriage, and three-linkage assembly, i.e., the boom, stick, and bucket.

The three linkage assembly is housed in the upper structure, which is supported by the undercarriage. The boom is connected to the upper structure with pin joints having horizontal rotation. The boom, stick and bucket assembly is also pi-jointed and operated with the use of hydraulic cylinders. The upper structure and the assembly together can swing against the undercarriage.
The whole hydraulic excavator can propel forward or backward. The attached coordinate frames indicate the possible motions of the components of the hydraulic excavator. Figure 2 shows a free body diagram of the stick during excavation, while Figure 3 shows bucket formation interaction.

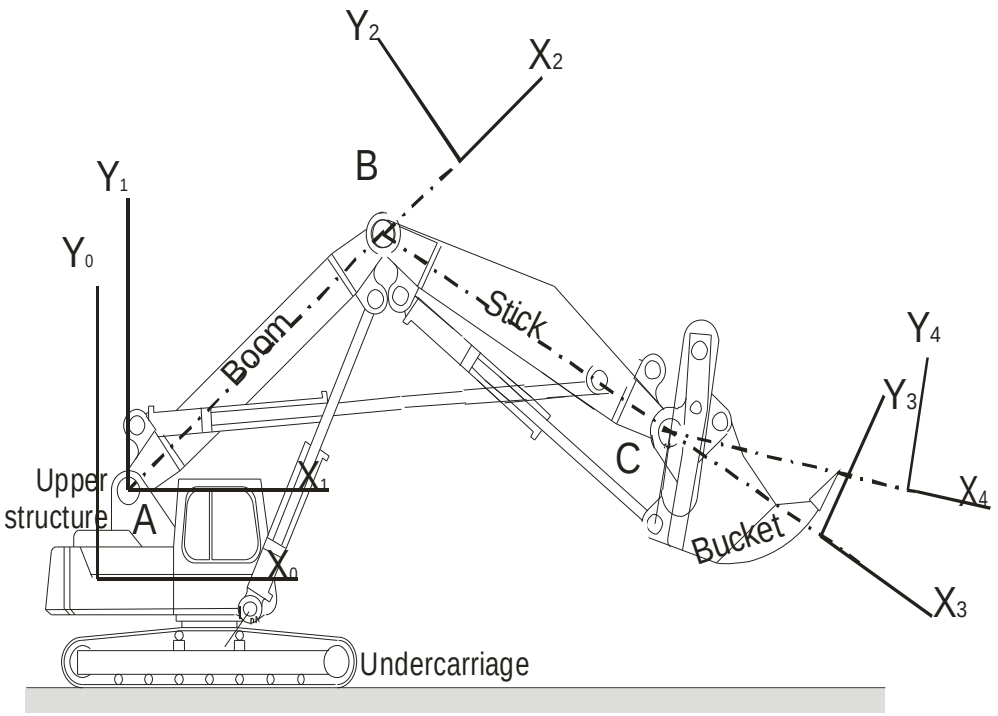

.

Figure 1 The hydraulic excavator

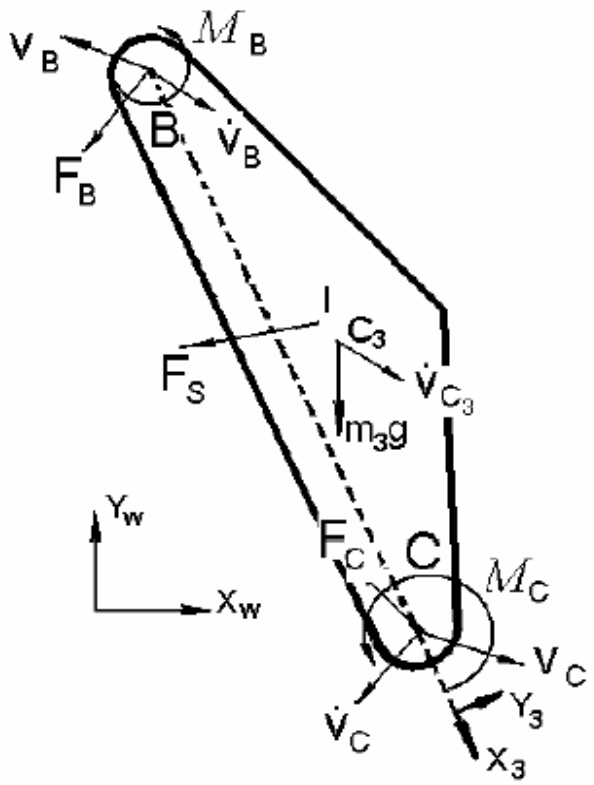

Figure 2 Free body diagram of the stick during excavation

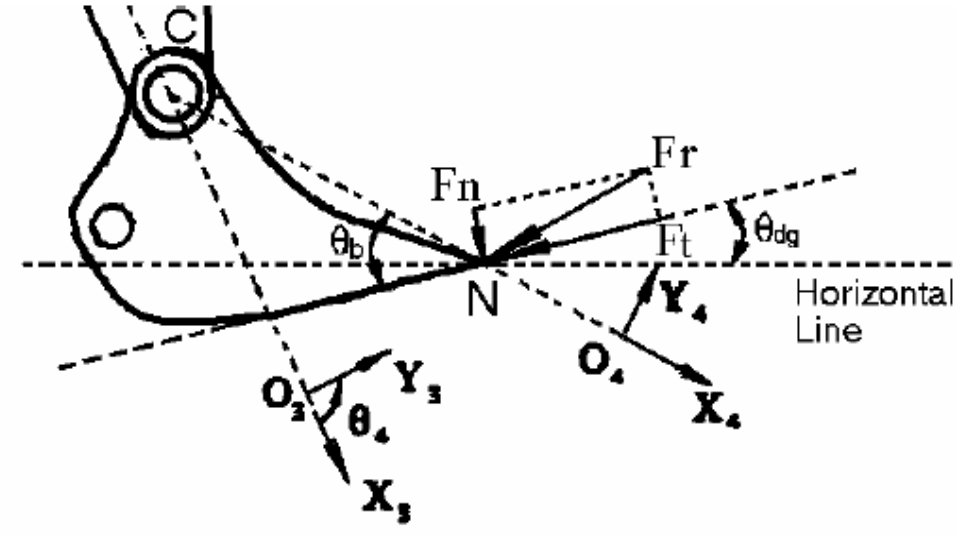

Figure 3 bucket-formation interaction

2.1 NEWTON-EULER METHOD

Between the two methods for describing the kinematics and dynamics of excavator excavators, Newton-Euler method is preferred over Lagrange one because it provides detailed information on all links and joints, which will be useful in the subsequent stress and/or performance analysis of the components during excavation [Koivo, et. al, 1996].

The focus on the boom, stick and bucket assembly of the hydraulic excavators because this research is only concerned with the digging section of a duty cycle. Therefore, the rotation of the upper structure is not modeled and the bucket, stick and boom assembly only moves on the vertical plane.

In Newton-Euler method, the velocities and accelerations are first computed iteratively for each link from boom to stick and then to bucket based on the kinematics of rigid bodies. From Figure 2 which shows a free body diagram of the stick during excavation, the unit vectors for the inertial reference frame are i,j and k and The only motion permitted is rotation about a fixed axis (z-axis), k. The kinematics equation for the stick are given as.

$$\vec{\omega}_C = \vec{\omega}_B + \left(\dot{\theta}_3\,\vec{k}\right)$$
$$\vec{\dot{\omega}}_C = \vec{\dot{\omega}}_B + \left(\ddot{\theta}_3\,\vec{k}\right) + \vec{\omega}_B \times \left(\dot{\theta}_3\,\vec{k}\right)$$
$$\vec{v}_C = \vec{v}_B + \left(\dot{\theta}_3\,\vec{k}\right) \times \vec{r}_{BC} \quad (1)$$
$$\vec{\dot{v}}_C = \vec{\dot{v}}_B + \vec{\dot{\omega}}_C \times \vec{r}_{BC} + \vec{\omega}_B \times (\vec{\omega}_B \times \vec{r}_{BC})$$

Where: $\vec{\omega}_B, \vec{\dot{\omega}}_B, \vec{\omega}_C, and\ \vec{\dot{\omega}}_C$ are the angular velocity and angular acceleration of the previous link the boom and stick, respectively. $\vec{v}_B, \vec{\dot{v}}_B, \vec{v}_C, and\ \vec{\dot{v}}_C$ are the translational velocity and translational acceleration at joint point B and C of the boom and stick, respectively. $\dot{\theta}_3$ and $\ddot{\theta}_3$ are the angular velocity and angular acceleration of the local coordinate system of the stick relative to that of the boom. The inertial force, ${}^3\vec{F}_3$ and moment, ${}^3\vec{M}_3$ acting on the stick can then be determined by applying the Newton-Euler's equation. The mathematical model in the local coordinate frame (about the gravitational center of the stick) is given by equation (2). m_3 and I_3 are the mass and inertial moment of the stick, respectively. From the free body diagram of the stick, all forces and moments are balanced resulting in the balance equation (3).

$${}^3\vec{M}_3 = I_3\vec{\dot{\omega}}_C + \vec{\omega}_C \times (I_3\vec{\omega}_C) \quad (2)$$
$${}^3\vec{F}_3 = m_3\vec{\dot{v}}_{C_3}$$
$$\vec{M}_B + \vec{M}_C + \vec{r}_{C_3B} \times \vec{F}_B + \vec{r}_{C_3B} \times \vec{F}_C + \vec{r}_{C_3I} \times \vec{F}_S = {}^3\vec{M}_3 \quad (3)$$
$$\vec{F}_B + \vec{F}_C + \vec{F}_S = {}^3\vec{F}_3$$

Where: $\vec{F}_B$and $\vec{F}_C$ are the forces acting on the stick from the boom and bucket, respectively, and expressed in the local coordinate frame. $\vec{F}_S$ is the hydraulic force exerted on the stick by the stick cylinder. $\vec{M}_B$ and $\vec{M}_C$ are the moments acting on the stick from the boom and bucket, respectively, and expressed in the local coordinate frame. The force balance equations can be established for the boom and bucket as well.

The complete set of the equations for describing the kinematics and dynamics of the boom, stick and bucket assembly involves near fifty equations, which can be solved for unknown parameters based on prescribed inputs. For

example, with a given digging trajectory and the digging force at the tip of the bucket, it is possible to calculate joint forces between links and hydraulic forces inside three cylinders, therefore, establishing the relations among the digging force, hydraulic forces and other factors [Alekseeva, et. al, 1985].

The interaction between the bucket and the excavated material is a complex problem and there are different models, which are applicable to different materials [Araya, et. al, 1988] and [Novak, A.J. 1991]. The resistive force, Fr as shown in Figure 3 was calculated using the model by [Alekseeva, et. al, 1985]:

$$F_r = k_p \left[k_s bh + \mu N + \varepsilon \left(1 + \frac{V_s}{V_b} \right) bh \sum_i \Delta x_i \right] \quad (4)$$

k_p and k_s are specific resistances in digging material; constants b and h are width and thickness of cut slice of the material, respectively; μ is the friction coefficient of the bucket and the cutting material; N is the pressure force of the bucket with the cutting material; ε is the coefficient of resistance experienced in filling the bucket during the movement of the prism of soil; V_s and V_b are volumes of the prism of cutting material and the bucket, respectively; and Δx_i is the increment along the horizontal axis. θ_b defines the angle between the foregoing plane that contains the bottom of the bucket and the X_4 -axis. The digging angle, θ_{dg}, is defined as the tangential angle of the proscribed trajectory with the horizontal line. With the time dependence of the trajectory known, the digging angles with time can be determined for each instant during the excavation process. F_t and F_n are the tangential and normal components of the resistive force.

Excavator performance is defined as power consumption of all cylinders during digging operation. The power delivered to each cylinder is the product of the force applied by that cylinder and the extension rate of this cylinder (assuming ideal hydraulic cylinders). Novak and Larson (1991) estimates the power delivered to the boom cylinder in equation (5).

$$P_b = \left| \vec{F}_b . \vec{V}_b \right| \quad (5)$$

$\overrightarrow{F_b}$ and $\overrightarrow{V_b}$ are the hydraulic force and extension rate of the boom cylinder, respectively. The total power required to drive the excavator is simply the sum of these individual powers:

$$P_{total} = \left| \overrightarrow{F_b} . \overrightarrow{V_b} \right| + \left| \overrightarrow{F_s} . \overrightarrow{V_s} \right| + \left| \overrightarrow{F_{bu}} . \overrightarrow{V_{bu}} \right| \quad (6)$$

$\overrightarrow{F_s}$ and $\overrightarrow{V_s}$ and $\overrightarrow{F_{bu}}$ and $\overrightarrow{V_{bu}}$ are the respective hydraulic forces and extension rates of the stick and bucket cylinders.

2.2 KANE METHOD

The basic components of the hydraulic excavator are shown in Figure 1. The global frame is *A* -$X_1Y_1Z_1$. Three local frame also are defined: the frame of *A*-$X_2Y_2Z_2$ is fixed to boom in point A; The frame of *B*-$X_3Y_3Z_3$ is fixed on stick in point B; and the coordinate system of *C*- $X_4Y_4Z_4$ is fixed to bucket in point C. From the structure shown in Figure 1, the transformation matrix of boom, stick, and bucket to base frame *A*-$X_1Y_1Z_1$ in origin *A* can be obtained as ${}^1_2A, {}^2_3A \; and \; {}^3_4A$ respectively . They are listed in the following.

$$ {}^1_2A = \begin{bmatrix} cos\,\theta_1 & -sin\,\theta_1 & 0 & 0 \\ sin\,\theta_1 & cos\,\theta_1 & 0 & 0 \\ 0 & 0 & 1 & 0 \\ 0 & 0 & 0 & 1 \end{bmatrix} \tag{7} $$

$$ {}^2_3A = \begin{bmatrix} cos\,\theta_2 & -sin\,\theta_2 & 0 & l_1 \\ sin\,\theta_2 & cos\,\theta_2 & 0 & 0 \\ 0 & 0 & 1 & 0 \\ 0 & 0 & 0 & 1 \end{bmatrix} \tag{8} $$

$$ {}^3_4A = \begin{bmatrix} cos\,\theta_3 & -sin\,\theta_3 & 0 & l_2 \\ sin\,\theta_3 & cos\,\theta_3 & 0 & 0 \\ 0 & 0 & 1 & 0 \\ 0 & 0 & 0 & 1 \end{bmatrix} \tag{9} $$

According to equations (7, 8 and 9), transformation matrix between each component to base frame can be obtain. And the ${}^1_3A, {}^1_4A$ present the matrix of boom, stick and bucket to base frame. These equations are also listed in following:

$$ {}^1_3A = {}^1_2A \cdot {}^2_3A = \begin{bmatrix} cos(\theta_1+\theta_2) & -sin(\theta_1+\theta_2) & 0 & l_1\,cos\,\theta_1 \\ sin(\theta_1+\theta_2) & cos(\theta_1+\theta_2) & 0 & l_2\,sin\,\theta_1 \\ 0 & 0 & 1 & 0 \\ 0 & 0 & 0 & 1 \end{bmatrix} \tag{10} $$

$$
{}^{1}_{4}A = {}^{1}_{2}A \cdot {}^{2}_{3}A \cdot {}^{3}_{4}A =
\begin{bmatrix}
cos(\theta_1+\theta_2+\theta_3) & -sin(\theta_1+\theta_2+\theta_3) & 0 & l_1 cos\,\theta_1 + l_2\, cos(\theta_1+\theta_2) \\
sin(\theta_1+\theta_2+\theta_3) & cos(\theta_1+\theta_2+\theta_3) & 0 & l_2 sin\,\theta_1 + l_1\, sin(\theta_1+\theta_2) \\
0 & 0 & 1 & 0 \\
0 & 0 & 0 & 1
\end{bmatrix} \quad (11)
$$

Where the l_1, l_2, l_3 are the length of boom, stick and bucket; $\theta_1, \theta_2, \theta_3$ are the angles of boom, stick and bucket respectively as Figure 1. According to the above transmission matrix, the global coordinates of each point in different component can be described. For example, for any point in bucket whose local coordinate value is (x_3,y_3), the values of global coordinate is given by equation (*12*)

$$
\begin{Bmatrix} X_3 \\ Y_3 \\ 0 \\ 1 \end{Bmatrix} =
\begin{bmatrix}
cos(\theta_1+\theta_2+\theta_3) & -sin(\theta_1+\theta_2+\theta_3) & 0 & l_1 cos\,\theta_1 + l_2\, cos(\theta_1+\theta_2) \\
sin(\theta_1+\theta_2+\theta_3) & cos(\theta_1+\theta_2+\theta_3) & 0 & l_2 sin\,\theta_1 + l_1\, sin(\theta_1+\theta_2) \\
0 & 0 & 1 & 0 \\
0 & 0 & 0 & 1
\end{bmatrix}
\begin{Bmatrix} x_3 \\ y_3 \\ 0 \\ 1 \end{Bmatrix} (12)
$$

Similarly, the global coordinates of point in boom or stick can be obtained by same method.

Based on above transformation matrix, inverse kinematics and forward kinematics can be studied. Forward kinematics analysis is to obtain trajectory of bucket tip or other points in components according to the angle of each joint in joint space. On the other hand, if the trajectory of bucket tip is known, the processing of solving joint angle is called inverse kinematics. In the two processes, the forward kinematics is simpler than inverse kinematics. In inverse kinematics analysis, solution of algebra equation is necessary. In most cases, the algebraic equations are nonlinear. In hydraulic excavator, neglecting motion of tract, equation (*12*) can be used to perform inverse kinematics analysis. If only the trajectory of tip is given, the angle of each joint is not unique. So another constraint of orientation of bucket should be added. It means that knowing the angle of $(\theta_1+\theta_2+\theta_3)$, the angle of $\theta_1, \theta_2, \theta_3$ can be determined. If the trajectory of bucket is given, the two angles and displacement must be fixed.

In hydraulic excavator, hydraulic cylinders are actuators to overcome the resistive force and drive components. These hydraulic cylinders form three kinematics constraint relationships as follows :

$$c_1{}^2 = \left(h_{1x}\cos\theta_1 - h_{1y}\sin\theta_1 - h_{ox}\right)^2 + \left(h_{1x}\sin\theta_1 - h_{1y}\cos\theta_1 - h_{oy}\right)^2 \quad (13)$$

$$c_2{}^2 = \left(l_1 + h_{21x}c_2 - h_{21y}s_2 - h_{12x}\right)^2 + \left(h_{21y}\sin\theta_2 - h_{21y}\cos\theta_2 - h_{12y}\right)^2 (14)$$

$$c_3{}^2 = \left(l_1 + l_1c_2 + h_{31x}c_{23} - h_{31y}s_{23} - h_{13x}\right)^2 \quad (15)$$

c_1 is the length of boom cylinder; c_2 is the length of stick cylinder; c_3 is the length of bucket cylinder; h_{ox} and h_{oy}, the coordinates value of a point on boom cylinder in undercarriage; h_{1x} and h_{1y}, the coordinate value of point of boom cylinder in undercarriage; h_{21x} and h_{21y}, the coordinate value of a point on stick cylinder in stick; h_{12x} and h_{12y}, the coordinate value of a point of stick cylinder in boom; h_{31x} and h_{31y} , the coordinate value of a point of bucket cylinder in bucket; h_{13x} and h_{13y}, the coordinate value of a point of bucket cylinder in boom. Based on transformation matrix, the velocities and accelerations can individually be derived. The bucket velocities and accelerations are:

$$\begin{bmatrix} X \\ Y \\ 0 \\ 1 \end{bmatrix}' = \begin{bmatrix} -\sin\theta_{123}\dot{\theta}_{123} & -\cos\theta_{123}\dot{\theta}_{123} & 0 & -l_1\sin\theta_1\dot{\theta}_1 - l_2\sin\theta_{12}\dot{\theta}_{12} \\ \cos\theta_{123}\dot{\theta}_{123} & -\sin\theta_{123}\dot{\theta}_{123} & 0 & l_1\cos\theta_1\dot{\theta}_1 + l_2\cos\theta_{12}\dot{\theta}_{12} \\ 0 & 0 & 1 & 0 \\ 0 & 0 & 0 & 1 \end{bmatrix} \begin{bmatrix} x \\ y \\ 0 \\ 1 \end{bmatrix} \quad (16)$$

$$\begin{bmatrix} X \\ Y \\ 0 \\ 1 \end{bmatrix}'' = \begin{bmatrix} -\sin\theta_{123}\ddot{\theta}_{123} - \cos\theta_{123}\dot{\theta}_{123}{}^2 & -\cos\theta_{123}\ddot{\theta}_{123} + \sin\theta_{123}\dot{\theta}_{123}{}^2 & 0 & a_1 \\ \cos\theta_{123}\ddot{\theta}_{123} - \sin\theta_{123}\dot{\theta}_{123}{}^2 & -\sin\theta_{123}\ddot{\theta}_{123} - \cos\theta_{123}\dot{\theta}_{123}{}^2 & 0 & a_2 \\ 0 & 0 & 1 & 0 \\ 0 & 0 & 0 & 1 \end{bmatrix}$$

(17)

Kane method is used to develop and analyze the structure of the static and dynamic problems associated with the hydraulic excavator. The process begins

with defining the general speeds u_1,u_2 ... u_n first; then the forces acting on the system are calculated, including external forces $(F_i)_j$, torques $(T_i)_j$, inertial forces $(F_i)_j{}^*$and inertial torques $(T_i)_j{}^*$. Then, the motion equations are formulated as in [Kane et al., 1983]:

$$F_r + F_r{}^* = 0 \tag{18}$$

where:

$$F_r{}^* = \sum_{i=1}^{m} \left[(F_i{}^*)_r \frac{\partial V_i}{\partial u_r} + (T_i{}^*)_r \frac{\partial W_i}{\partial u_r} \right]$$

$$F_i{}^* = -m_i a_i \; ; T_i{}^* = -I_i \varepsilon_i \quad ; \; F_r = \sum_{i=1}^{m} \left[(F_i)_r \frac{\partial V_i}{\partial u_r} + (T_i)_r \frac{\partial W_i}{\partial u_r} \right]$$

The general speeds are given as: u_1, u_2, u_3:, where $u_1 = \dot{\theta}_1$, $u_2 = \dot{\theta}_2$ $u_3 = \dot{\theta}_3$. Then we can solve the partial velocity for different velocities. For example, for the points in the bucket, the partial velocities are shown as follows :

$$\frac{\partial v_3}{\partial \dot{\theta}_i} = \begin{bmatrix} -sin\,\theta_{123} & -cos\,\theta_{123} \\ cos\,\theta_{123} & -sin\,\theta_{123} \end{bmatrix} \begin{Bmatrix} x \\ y \end{Bmatrix} + \begin{bmatrix} -sin\,\theta_{12} & -cos\,\theta_{12} \\ cos\,\theta_{12} & -sin\,\theta_{12} \end{bmatrix} \begin{Bmatrix} l_2 \\ 0 \end{Bmatrix} + \begin{bmatrix} -sin\,\theta_1 & -cos\,\theta_1 \\ cos\,\theta_1 & -sin\,\theta_1 \end{bmatrix} \begin{Bmatrix} l_1 \\ 0 \end{Bmatrix} \tag{19}$$

Differentiating equation (*13,14 and 15*), the relationship between the velocities of cylinder and linkage angle can be obtained as shown below :

$$\frac{\partial \dot{c_1}}{\partial \dot{\theta_1}} = \frac{1}{c_1} \left[h_{0x}(h_{1x}s_1 + h_{1y}c_1) - h_{0y}(h_{1x}c_1 + h_{1y}s_1) \right] \tag{20}$$

$$\frac{\partial \dot{c_2}}{\partial \dot{\theta_2}} = \frac{1}{c_2} \left[(l_1 - h_{12x})\,(-h_{12x}s_2 - h_{21y}c_2) - h_{12y}(h_{21y}c_2 - h_{21y}s_2) \right] \tag{21}$$

$$\frac{\partial \dot{c_3}}{\partial \dot{\theta_2}} = \frac{1}{c_3} \left[(l_1 - h_{13x})\,(-l_2s_2 - h_{31x}s_{23} - h_{31y}c_{23}) + (-h_{13y})(l_2c_2 + h_{31x}c_{23} - h_{31y}s_{23}) \right] \tag{22}$$

h_{21x} and h_{21y} are coordinate values of a point of arm cylinder in stick.

The entire external forces incident on the excavator are included in developing the system static model. These forces include the hydraulic force

from cylinders, gravity of the handle, the payload for digging resistance and gravity of material as shown below.

$$T_1 \frac{\partial \dot{c_1}}{\partial \dot{\theta_1}} + \vec{F} \frac{\partial \vec{s_1}}{\partial \dot{\theta_1}} + M_1\, g(x_1 cos\, \theta_1 - y_1 sin\, \theta_1) + M_2\, g(l_1\, cos\, \theta_1 + x_2\, cos\, \theta_{12} - y_2\, sin\, \theta_{12}) + M_3\, g(l_1\, cos\, \theta_1 + l_1\, cos\, \theta_{12} + x_3\, cos\, \theta_{123} - y_{23}\, sin\, \theta_{123}) = 0 \quad (23)$$

$$T_2 \frac{\partial \dot{c_2}}{\partial \dot{\theta_2}} + T_3 \frac{\partial \dot{c_3}}{\partial \dot{\theta_2}} + \vec{F} \frac{\partial \vec{s}}{\partial \dot{\theta_2}} + M_2\, g(x_2\, cos\, \theta_{12} - y_2\, sin\, \theta_{12}) + M_3\, g(l_2\, cos\, \theta_{12} + x_3\, cos\, \theta_{123} - y_3\, sin\, \theta_{123}) = 0 \quad (24)$$

$$T_3 \frac{\partial \dot{c_3}}{\partial \dot{\theta_3}} + \vec{F} \frac{\partial \vec{s}}{\partial \dot{\theta_3}} + M_3\, g(x_3 \cos\theta_{123} - y_3 \sin\theta_{123}) = 0 \quad (25)$$

According to above static equations, some physical significance of items can be studied. The three equations are corresponding to three general speed u_1, u_2 *and* u_3.

Therefore, $T_1 \frac{\partial \dot{c_1}}{\partial \dot{\theta_1}}$; $T_2 \frac{\partial \dot{c_2}}{\partial \dot{\theta_2}} + T_3 \frac{\partial \dot{c_3}}{\partial \dot{\theta_2}}$ and $T_3 \frac{\partial \dot{c_3}}{\partial \dot{\theta_3}}$ are the driving torques to $\theta_1, \theta_2,$ *and* θ_3. For torque $T_1 \frac{\partial \dot{c_1}}{\partial \dot{\theta_1}}$, $\frac{\partial \dot{c_1}}{\partial \dot{\theta_1}}$ is the arm force. Similarly, the contribution of different forces as resistant force, gravity of material and components on whole system can be analyzed.

2. SIMULATION

In order to study the effect of different parameters on the performance of a hydraulic excavator, a parameterized virtual model in SIMULATION-X [Klein et al., 2004], simulation environment was developed. By examining the effect of different parameters and different values for each parameter, the optimized combination for the hydraulic excavator performance could be found.

Three different initial conditions are considered to start and run the simulator:

a. Force conditions: The hydraulic force inputs to the cylinders and the digging force to the tip of the bucket are applied and the time response of the system is then obtained by measuring the displacement, velocity and acceleration of each joint and the extension displacement, extension velocity and extension acceleration of each cylinder.

b. Displacement condition: A digging trajectory at the bucket tip is prescribed as input. The model solves for the required displacement input for each cylinder to achieve that trajectory. It also output other parameters such as joint angles, angular velocity and acceleration.
c. Mixed condition: The extension displacement of each cylinder combined with a prescribed resistive force at the bucket tip is prescribed as the input. With the time dependence of the extension displacement of each cylinder and the resistive force known, the hydraulic force inside each cylinder and joint force between two links can be evaluated.
d. Other assumptions are:

(i) there is no joint friction between the upper structure and the assembly and between the links within the assembly; and
(ii) the hydraulic cylinders are ideal, i.e., no frictional losses

Figure 4 shows a hydraulic excavator simulator developed in SIMULATION-X environment. Figure 5 shows 3D solid hydraulic excavator model, while Figure 6 shows a virtual prototype. Only the front-end assembly including boom, stick and bucket of the hydraulic excavator is modeled for the reason described in the previous section.

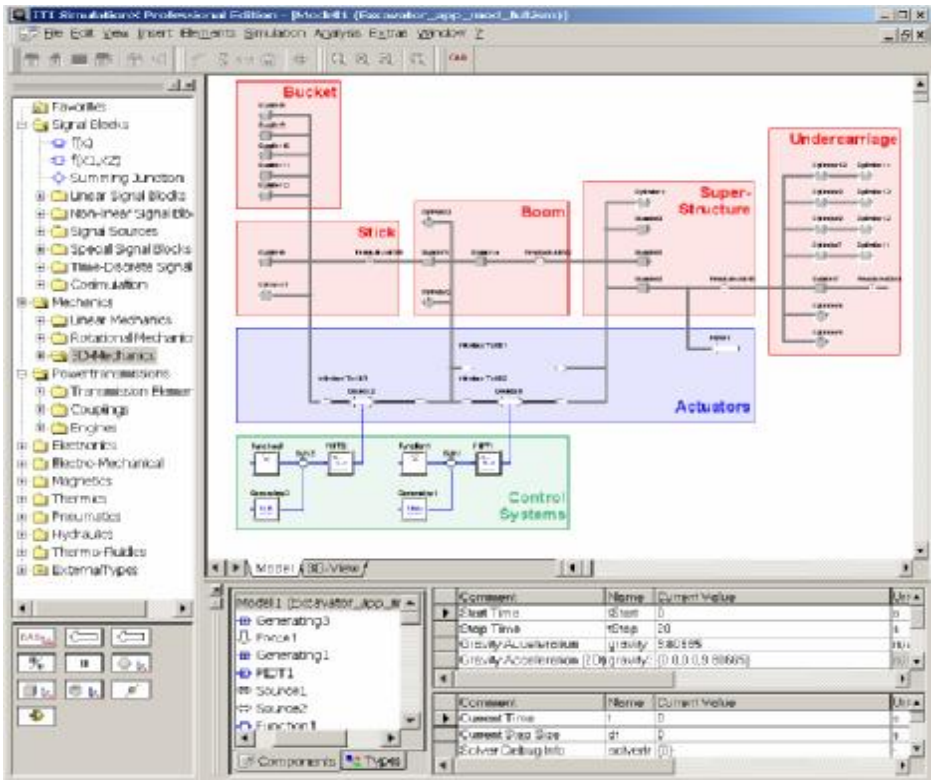

Figure 4 A Hydraulic Excavator in SIMULATION-X Simulation Environment

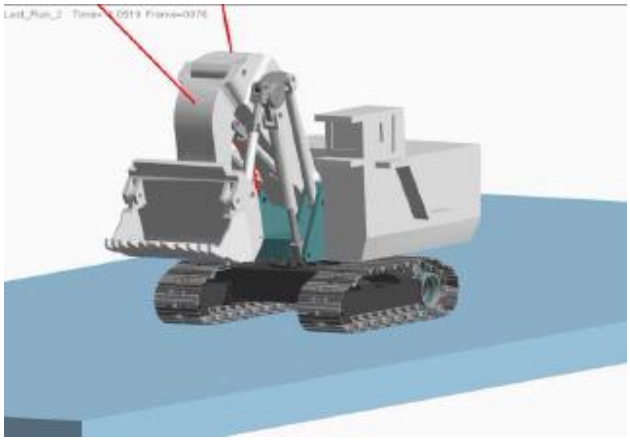

Figure 5 3D solid hydraulic excavator model

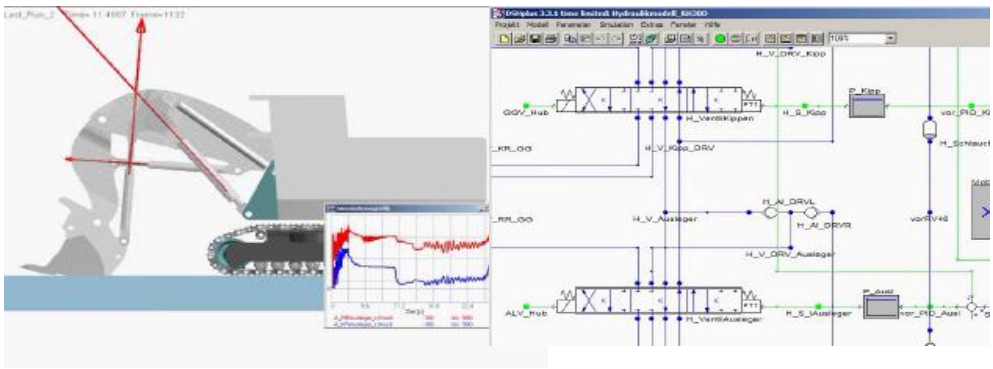

Figure 6 Virtual prototype for hydraulic excavator

3.1 TEST EXAMPLES

Examples are included to illustrate the performance of hydraulic excavator based on given digging paths and to define efficient digging profiles based on energy consumption.

The kinematics and dynamic simulations of hydraulic excavator are illustrated by prescribing an assumed trajectory at the bucket tip when excavating a formation or muck-pile (as illustrated in Figure 7). The formation or muck-pile has a slope of 50 degrees. The trajectory is designed such that at

the end of its execution, the volume of the cut material is equal to the bucket capacity of the excavator. The bucket tip moves at constant speed and it takes 7.5 seconds to execute the entire trajectory. The main geometry data for the excavator simulated is listed in Table 1, while the parameters for determining the resistive force are shown in Table 2.

Table 1. Main Hydraulic Shovel Data [Alaydi, 2008]

	Length[1] *(m)*	Mass *(kg)*	Inertia Moments[2] *(Kg. m^2)*
Boom	7.682	36420	1.850E + 005
Stick	5.334	21310	4.810E + 004
Bucket	3.950	40800	4.567E + 004
Bucket capacity 5.625m^3			

[1]Length between two joints for boom and stick and between joint and bucket tip for bucket
[2]Moment of inertia about the gravitational center

Table 2: Data for Excavated Material Properties [Luengo, 1988]

k_p	1.005	ε	55.000 *kg /(m^2 / s^2)*
k_s	5.500		
μ	0.1	*b*	4.8 *m*
N	1 *kg . m/s^2*		

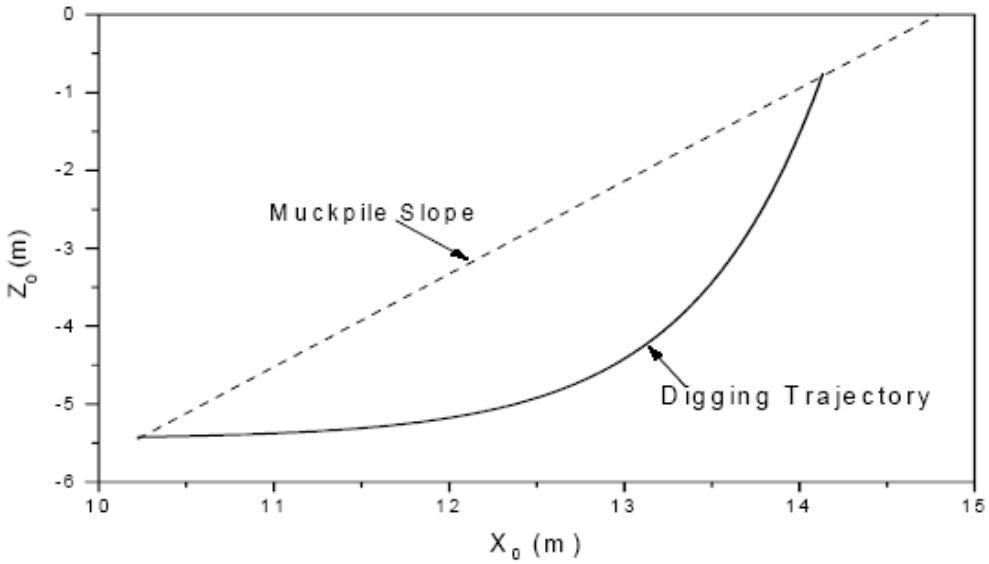

Figure 7 Trajectory for the bucket tip

Given the geometrical and physical parameters for the excavator and the cutting material, the evolution of the joint angles and cylinder forces with time are shown in Figures 8 and 9 based on the given trajectory curve. Figure 9 shows that the cylinders experience three phases during the digging part: a gradual increase, reaching maximum and gradual decrease. The force reaches its maximum around the middle of the trajectory.

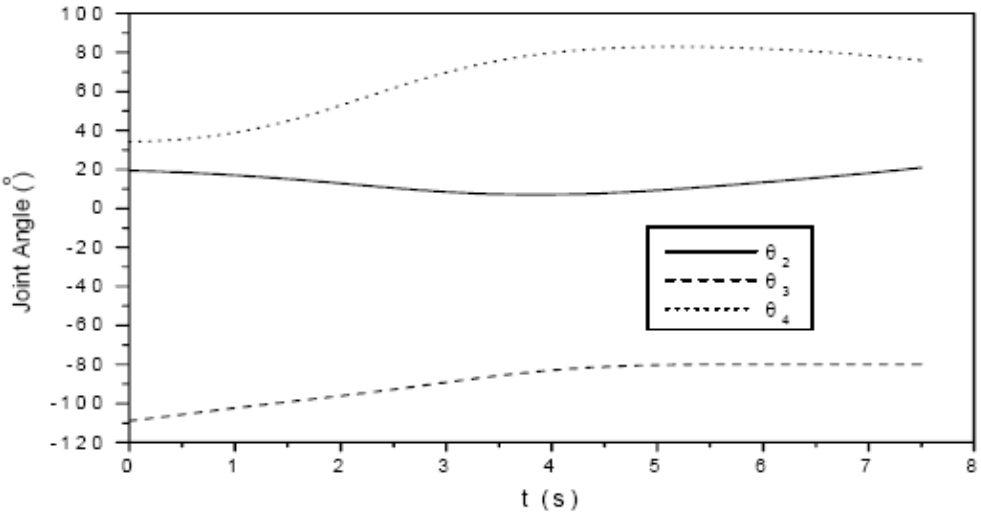

Figure 8 Changing joint angle with time during excavating

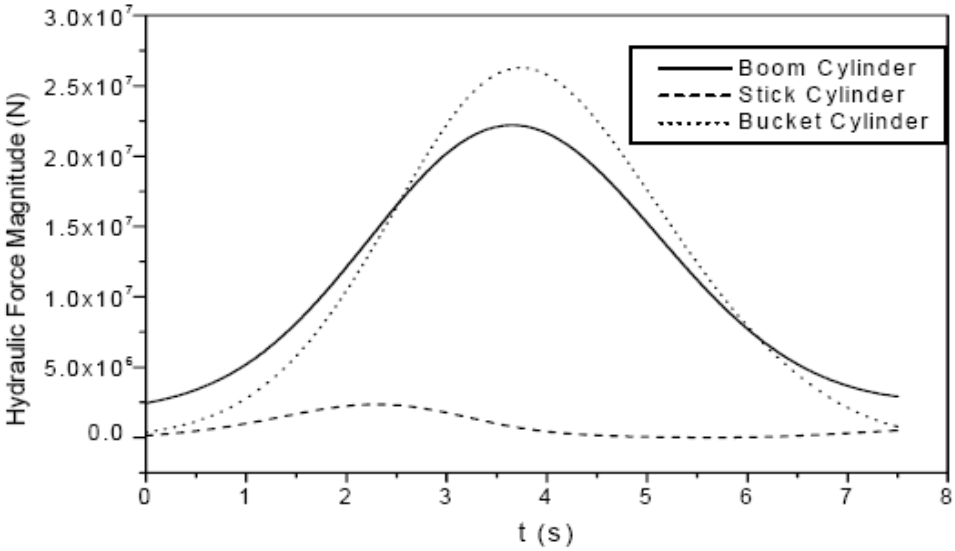

Figure 9 Force changing with time during excavating

It is often required in surface mining industry that the duty cycle is shortened in order to improve production efficiency. This is particularly important for large-scale operations where excavators are over-trucked. Even reducing the execution time of a single cycle of an operation by a few seconds can translate into large savings over the entire job.

The same trajectory as shown in Figure 7 is completed within three different digging times: 5, 7.5 and 10 seconds. The power consumption for the three different times are simulated as shown in Figure 10. It can be seen that shortening the digging time consumes more energy. The peak power required almost doubles when the digging time is reduced by half. Therefore, there is a need for a trade-off between energy consumption and saving duty cycle.

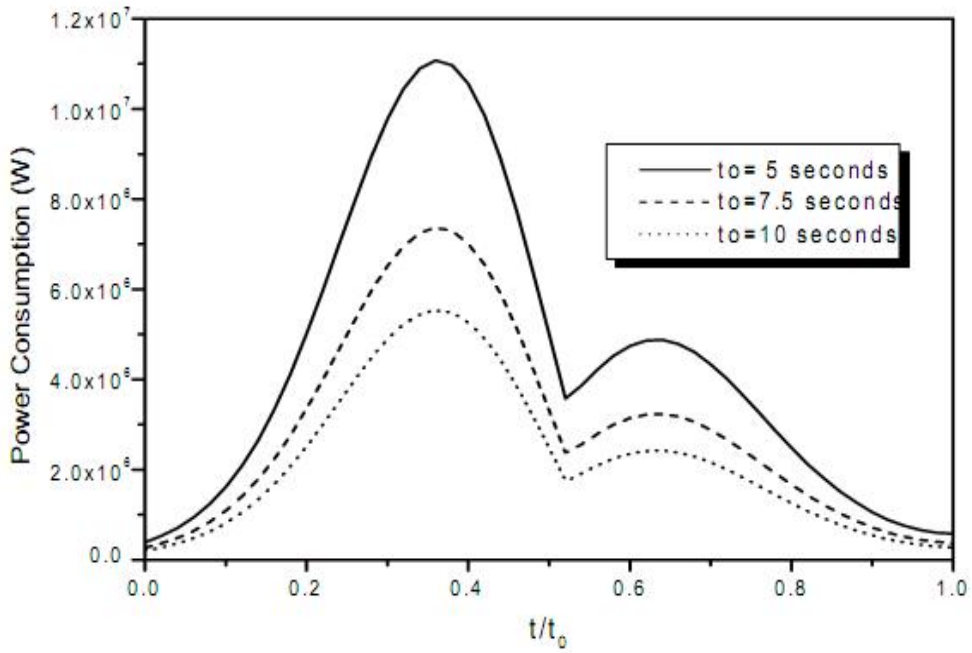

Figure 10 Trajectory power consumption for the three different excavating time

Digging trajectory is a very important factor that influences the performance of a hydraulic excavator. As indicated by Hendricks et al (1989), the excavator response may be more heavily dependent on the position of the

bucket in the material rather than the material characteristics. Three different trajectories are considered with the end point on each trajectory being reached at the same time of 7.5 seconds and with full bucket loading capacity. The digging trajectories are shown in Figure 11.

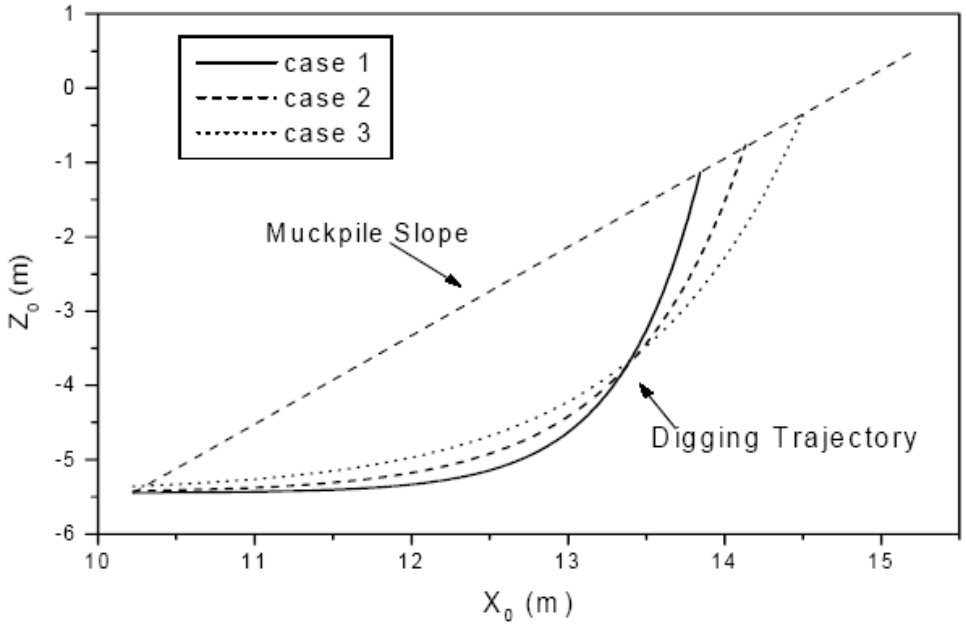

Figure 11 Three trajectories for bucket tip of hydraulic excavator

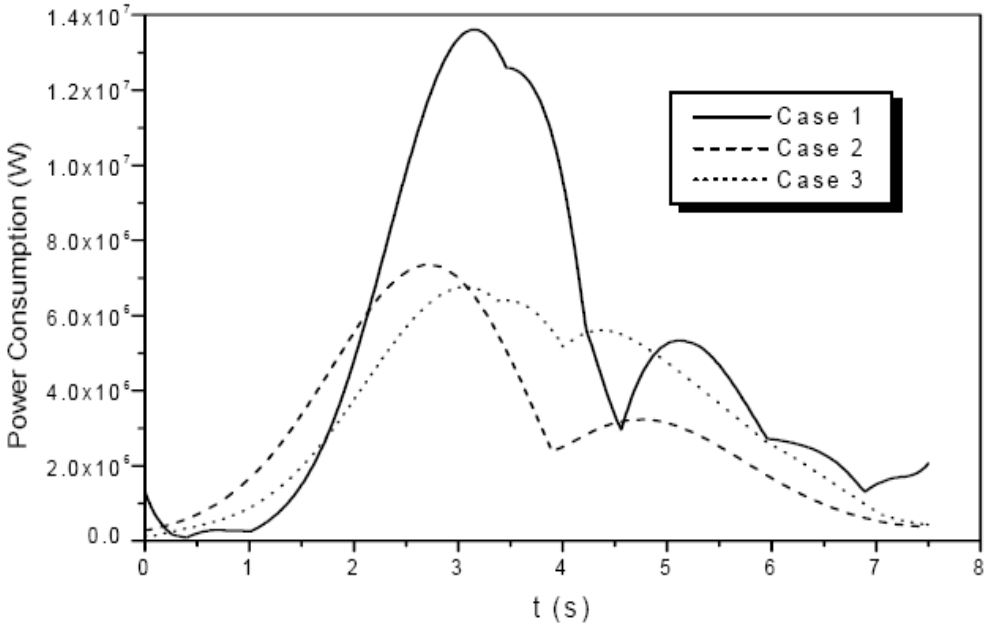

Figure 12 Corresponding power consumption for the trajectories

The corresponding power consumption for the trajectories are shown in Figure 12 (case 1 corresponds to the trajectory with short but deep digging, case 3 with long but shallow digging and case 2 in between the first two cases). It can be seen that a short but deep trajectory (case 1) requires more power consumption than a long but shallow one. The peak power required decreases by 50% when the shallow digging trajectory is executed instead of the deep one.

3. CONCLUSIONS

In this paper, transformation matrix method is used to describe the motion of machine and analyze the kinematics relationship; then Kane method is applied to build static and dynamic model in closed form.

Analysis of the excavator was performed applying the Newton-Euler equations and Kane method.

Hydraulic excavator simulators for surface mining were developed using SIMULATION-X simulation environment. The parameterized characteristics

of the simulator make it easy to investigate the effect on excavator performance under varying working conditions. The simulator captures the kinematics and dynamics of the excavator within its operating environment, this parameterized simulator provides a powerful tool for performance monitoring, excavation process designs and structural optimization of excavators. Simulator also enables a virtual prototyping environment for complex mechanical systems and performing detailed analysis before detailed design and/or manufacturing to minimize the use of costly physical prototypes. The virtual prototyping technique may also be useful in improving design quality and dramatically reducing product development time. The results of this paper are extremely important, since they can influence further technology development in the mining field.

Based on results of this paper, it can be concluded that changes in parameters such as digging time or trajectory influence the performance of hydraulic excavators, as indicated by different power consumptions for different digging times and different digging trajectories. A shortened digging time increases the power required for the. The peak power required almost doubles when the digging time reduces half. The simulation on the effect of different digging trajectories also shows that a shallow trajectory consumes less power than a deep trajectory when the two trajectories are traveled within the same time duration. The peak power required decreases about 50% when the shallow digging trajectory is executed instead of the deep one. This paper indicates energy savings if proposed technology would be applied

This paper advances knowledge and frontiers in excavator excavation, and provides a basis for the Intelligent Excavators Technology (IET) to solve the problems associated with material excavation.

4. REFERENCES

[1] Kane, T. and Levinson. D.1985. Dynamics: Theory and Applications. McGraw-Hill, NY.

[2] lmanishi, E., Zui, H., Yoshimatsu, H. and Niwata, K., 1987. Study on simulation of linkage mechanism. Transactions of the Japan Society of Mechanical Engineers, Vo1.53, No.492, p.1711-1719.

[3] Shishaev, S. and Mochalov, E., 1989. Evaluating the characteristics of the working process of a hydraulic power excavator with an active dipper. Soviet Mining Science, Vo1.24, No.5, p.452-457.

[4] Daneshmend, L., Hendricks C., Wu S., and M. Scoble. 1993. Design of a Mining Shovel Simulator. Mine Design for 21st Century, Bawden & Archibald (Ed.). Balkema, Rotterdam.
[5] Tafazoli, S., Lawrence P., and Salcudean S.E.. 1999. "Identification of Inertial and Friction Parameters from Excavator Arms". IEEE Trans. on Robotics and Automation, Vol. 15, No.5, p.966-971.
[6] Murray, R., Li Z. and Sastry S. 1993. A Mathematical Introduction to Robotic Manipulation. CRC Press, Boca Raton, USA.
[7] Haug, E.J. 1989. Computer Aided Kinematics and Dynamics of Mechanical System, Volume I: Basic Methods. Allyn and Bacon, Boston.
[8] Frimpong, S., Hu Y. and Szymanski J. 2002. "Dynamic Shovel Excavation Simulator in Surface Mining Operations". Summer Computer Simulation Conference, SCSC 2002 Proc. San Diego, CA, July p.14-19 (CDROM)
[9] Frimpong, S., Hu Y. and Chang Z. 2003. "Hydraulic Shovel Simulator in Surface Mining Excavation Engineering". 12th International Symposium on Mine Planning & Equipment Selection, MPES, Kalgoorlie, West Australia, April p.23-25 (CDROM).
[10] Koivo, A., 1994. Kinematics of excavators (backhoes) for transferring surface materials. Journal of Aerospace Engineering, Vol.7, No.1, p.17-32.
[11] Blouin, S., Hemami, A. and Lipsett, M., 2001. Review of resistive force models for earthmoving processes. Journal of Aerospace Engineering, Vo1.14, No.3, p.102-111.
[12] Koivo, A., Thoma, M., Kocaoglan, E. and Rade-Cetto , J., 1996. Modeling and control of excavator dynamics during digging operation. J. Aerospace Eng., Vo1.9, No.1, p.10-18.
[13] Alaydi Juma Yousuf, 2008. Mathematical Modeling of Pump Controlled System for Hydraulic Drive Unit Of Single Bucket Excavator Digging Mechanism. Jordan Journal of Mechanical and Industrial Engineering Vol.2, No.3, p.157 – 162.
[14] Alekseeva, T., Artemev, K., Voitsekhouskii, R., and Ulyanov, N., 1985. Machines for earthmoving work, theory and calculations. Amerind Publishing Co., New Delhi, India.

[15] Araya, H., Kakuzen, M., Kimura, N. and Hayashi, N., 1988. Automatic control system for hydraulic excavators. Proceedings of the USA-Japan Symposium on Flexible Automation - Crossing Bridges: Advances in Flexible Automation and Robotics. Minneapolis, MN, USA, p.695-701.

[16] Novak, A. and Larson, C., 1991. A computer simulation of backhoe type excavators. International Off-Highway and Power plant Congress and Exposition, SAE SP-884, Milwaukee, Wisconsin, USA, p.41-48.

[17] Tafazoli, S., Lawrence P., and Salcudean S., 1999. Identification of Inertial and Friction Parameters from Excavator Arms. IEEE Trans. on Robotics and Automation, Vol.15, No.5, p.966-971.

[18] Luengo, O, Singh, S. and Cannon, H., 1998. Modeling and identification of soil-tool interaction in automated excavation. Proceedings of the 1998 IEEE/RSJ International Conference on Intelligent Robots and Systems, Victoria, BC, Canada, p.1900-1906.

[19] A. Klein, U., D. Sanders, ITI SimulationX and Komatsu Mining Germany, March 2004. Mechatronics - a New Challenge for Hydraulic Simulation. Proceedings of the 4th International Fluidpower Conference "Intelligent Solutions by Fluid Power". Dresden, Germany